

Non-Locality of Experimental Qutrit Pairs

C Bernhard[†], B Bessire[†], A Montana^{*}, M Pfaffhauser^{*},
A Stefanov[†], S Wolf^{*}

[†] Institute of Applied Physics, University of Bern, Bern, Switzerland.

^{*} Faculty of Informatics, USI Lugano, Switzerland.

Abstract. The insight due to John Bell that the joint behavior of individually measured entangled quantum systems cannot be explained by shared information remains a mystery to this day. We describe an experiment, and its analysis, displaying non-locality of entangled qutrit pairs. The non-locality of such systems, as compared to qubit pairs, is of particular interest since it potentially opens the door for tests of bipartite non-local behavior independent of probabilistic Bell inequalities, but of deterministic nature.

1. Non-Locality in Theory . . .

The discovery of *John Bell* that nature was non-local and quantum physics cannot be embedded into a local realistic theory in which the outcomes of experiments are completely determined by values located where the experiment actually takes place, and no far-away variables, is profound. It probably poses more questions than it has solved: If shared classical information [4] as well as hidden communication [3] both fall short of explaining non-local correlations, what “mechanism” could possibly be behind this strange effect? What can we learn from Bell’s insight — and from the series of experiments carried out in the aftermath [18, 2, 28, 30] — about the nature of space and time? What can we conclude about free choices (randomness) and, more generally, the role of *information* in physics and in our understanding of natural laws? In fact, Bell’s theorem is an *information-theoretic* statement: It characterizes what kind of joint input-output behavior

$$P(ab|xy)$$

can in principle be explained by shared (classical) information R , i.e., is of the form

$$\sum_r P_R(r) P^r(a|x) P^r(b|y) ,$$

and which cannot. The relationship to (quantum) physics is given by the fact that the joint behavior — where the inputs are given by the choice of the measurement settings and the output is the measurement outcome — of two (or more) parts of some entangled system are non-local, i.e., violate a *Bell inequality*. Bell inequalities are linear constraints that all local systems satisfy and that, in their totality, define the *local polytope* in the space of *non-signaling systems*, the latter being all behaviors not allowing for the transmission of information.

In this article, an experiment is described in which entangled three-dimensional systems are generated and measured, and it is analyzed whether non-local behavior can be observed. More precisely, the experiment, and its analysis, deals with maximally as well as partially entangled qutrit pairs. One of the questions of interest is whether maximal entanglement also means maximal non-locality. Hereby, the strength of non-locality is measured not only by the extent of a Bell inequality violation, but also in terms of the distance to the local polytope, as well as a novel method based on the amount of *communication* required for classically simulating the behavior observed experimentally.

The experimental realization of entangled qutrit pairs as opposed to qubit pairs is of interest for several reasons. One of them is that in principle, non-local correlations directly based on impossible colorings, i.e., the Kochen/Specker theorem [22], become possible [24]. This type of non-local behavior is conceptually simpler since it does not depend on probabilities, but is deterministic in nature.

2. ... and Experiment

Due to the extremely weak interaction with their environment, photons exhibit strong resistance against decoherence and can, therefore, be transmitted over large distances without altering their state. Photonic quantum states are thus ideal systems to carry out tests of non-locality with entangled states. Moreover, photons entangled in their polarization, momentum, or energy-time degrees of freedom can be experimentally generated by non-linear processes and coherently controlled and modified through linear optics. In the context of non-locality tests, the experimental study of entangled photonic states started in 1972 with the observation of non-classical correlations in the polarization of two photons emitted in an atomic cascade from a calcium atomic effusive beam [18]. This type of source was further improved and an experiment was performed in 1982 where the changes of the analyzers' orientation and the detection on each side were separated by a spacelike interval [2]. This experiment showed a statistically significant violation of Bell's inequality, demonstrating the non-locality of nature at its fundamental level. Since then, non-locality has been tested by numerous experiments which all confirmed the predictions of quantum mechanics under different conditions. Theories reconciling the quantum collapse and Lorentz invariance have been tested [27]. Further, boundaries on the speed of a potential superluminal influence have been experimentally set [26]. Entanglement between photons was shown to be conserved over distances on the order of kilometers in optical fibers [28] or in free-space [29]. Ongoing research is oriented towards experiments between ground station and low-orbit satellites.

Much effort is nowadays put into the closure of possible loopholes which can distort the outcomes of Bell test measurements. The presence of loopholes allows to explain the measurement results by a local theory even if a measured violation of a Bell inequality pretends the existence of non-classical correlations. Apart from space-time separation between the measurement devices (the communication loophole), the most studied loophole is the so called detection loophole. This loophole can be closed using detectors with sufficiently high efficiencies. Massive particles like ions or atoms can be detected with an efficiency of almost unity [25], however, have not yet been detected in a spacelike separated configuration [20]. Photons are nowadays detected with high efficiency in Bell experiments using super-conducting single photon detectors [19].

The locality condition is very difficult to be fully satisfied without any additional

hypothesis on the theory to be tested. It requires that the choices of the measurement settings have to be realized without any possible local causal relation between them. The most independent choices would be that Alice and Bob freely chose the settings themselves. The same applies for the detection of the measurement results. Because the measurement problem is still not solved in quantum mechanics, the detection should be considered to occur at the instant when Alice and Bob have conscience of the outcome result. In both cases the reaction times of Alice and Bob would require to perform the experiment over distances larger than the earth's diameter.

Most of the experiments mentioned here were carried out with photon pairs in entangled qubit states. Their non-locality was revealed by violating a Bell inequality, for instance the CHSH inequality [12], given by

$$I_2 \leq 2 . \quad (1)$$

In the following, we let A_x , with $x = 1, 2$, be an operator measured by Alice and B_y , with $y = 1, 2$, be an operator measured by Bob. The Bell parameter I_2 is then expressed as

$$I_2 = |P(A_1 = B_1) - P(A_1 \neq B_1) + P(A_1 = B_2) - P(A_1 \neq B_2) - P(A_2 = B_1) + P(A_2 \neq B_1) + P(A_2 = B_2) - P(A_2 \neq B_2)| , \quad (2)$$

and the outputs a and b are restricted to $a, b = 0, 1$. The maximal violation of Eq. (1), together with the corresponding measurement settings, can be fully determined by means of the two-qubit density matrix and the algorithm provided in [21]. The maximal violation of the CHSH inequality is achieved for a maximally entangled state given by

$$|\psi\rangle^{(2)} = \frac{1}{\sqrt{2}}(|0\rangle_A |0\rangle_B + |1\rangle_A |1\rangle_B) . \quad (3)$$

However, nothing restrains us from using pairs of photons entangled in more-than-two-dimensional spaces. While the polarization of light only carries two orthogonal states, the other modes of light, energy, and transverse momentum, can in principle encode much larger dimensions. Whereas the behavior of entangled qubits is fully characterized, their extensions to higher dimensions, denoted as qudits, are far from having been fully studied. A first approach to examine the non-classical correlations between two entangled qudits is to consider these states in the context of a new family of Bell inequalities introduced by Collins *et al.* (hereafter referred to as CGLMP) in [13].

2.1. Bell inequality for entangled qutrits

In the following, we focus on a two-qutrit state

$$|\psi\rangle^{(3)}(\gamma) = \frac{1}{\sqrt{2+\gamma^2}}(|0\rangle_A |0\rangle_B + \gamma |1\rangle_A |1\rangle_B + |2\rangle_A |2\rangle_B) \quad (4)$$

with a variable degree of entanglement γ .

In order to experimentally investigate the non-local properties of the state (4) we make use of the CGLMP inequality for $d = 3$ given by

$$I_3 \leq 2 \quad (5)$$

with the corresponding Bell parameter

$$I_3 = |P(A_1 = B_1) + P(B_1 = A_2 + 1) + P(A_2 = B_2) + P(B_2 = A_1) - P(A_1 = B_1 - 1) - P(B_1 = A_2) - P(A_2 = B_2 - 1) - P(B_2 = A_1 - 1)|. \quad (6)$$

For $d = 3$, we have measurement outcomes $a, b = 0, 1, 2$. At first sight, it seems to be intuitive that a maximally entangled state leads to the highest violation of a Bell inequality. However, for entangled qudits with $d > 2$, there exists theoretical evidence that non-maximally entangled qudits reach higher violations of the CGLMP inequality than maximally entangled states [1, 33]. In fact, it was shown that Eq. (5) is maximally violated for $\gamma = \gamma_{max} \approx 0.792$. To experimentally determine $I_3(\gamma)$, we exploit energy-time entangled photons to encode entangled two-qutrit states according to Eq. (4).

2.2. Experiment

We use an experimental setup in which energy-time entangled photons are generated by means of a spontaneous parametric down-conversion (SPDC) process induced by a quasi-monochromatic pump laser. It can be shown with numerical methods [32] that in this case, the entanglement content in the generated two-photon state is potentially very high by calculating an entropy of entanglement of $E = (21.1 \pm 0.2)$ ebits.

The experimental arrangement shown in Figure 1 is subdivided into three parts: The SPDC crystal prepares entangled two-photon states whose spectrum is discretized with a spatial light modulator (SLM) to generate entangled qudits. The ability of the SLM to individually control the amplitude and phase of selected spectral components then allows to manipulate the qudit states. Finally, the photons are detected in coincidence through sum-frequency generation (SFG) in a second non-linear crystal.

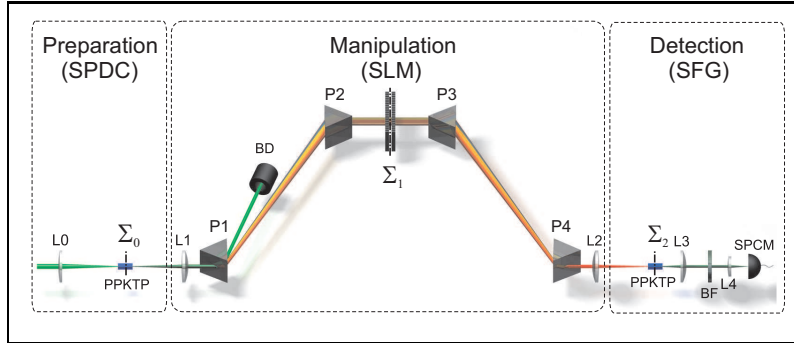


Figure 1. Overview of the experimental setup. Preparation: L0 pump beam lens with focal length $f = 150$ mm, PPKTP non-linear crystal for SPDC. Manipulation: BD beam dump, SLM spatial light modulator, symmetric two-lens (L1, L2) imaging arrangement ($f = 100$ mm) with a (de)magnification factor of six, P1-P4 four-prism compressor. Detection: PPKTP non-linear crystal for SFG, BF bandpass filter, SPCM single photon counting module with a two-lens (L3, L4) imaging system. Imaging planes are denoted with Σ_k .

To prepare entangled photon pairs degenerated at 1064 nm, we pump a $L_{DC} = 11.5$ mm long and periodically poled KTiOPO_4 (PPTKP) crystal with a poling periodicity of $G_{DC} = 9 \mu\text{m}$. The pump laser is a quasi-monochromatic Nd:YVO_4 (Verdi) laser centered at 532 nm featuring a narrow spectral full width half maximum

of about 5 MHz. The collinear pump beam is focused into the middle of the PPKTP crystal (Σ_0) with a power of 5 W. The down-conversion crystal is mounted in a copper block whose temperature is stabilized to ± 0.1 °C. The operating temperature of the PPKTP crystal is chosen for collinear emission and, according to type-0 SPDC, all involved photons are identically polarized. This configuration leads to a spectral width of $\Delta\lambda_{DC} \approx 105$ nm around 1064 nm which implies a spectral mode density of $n \approx 0.2$ entangled pairs per mode [16]. Therefore, we operate below the single photon limit, and thus in the quantum regime, where the entangled pairs are temporally well separated from each other. The corresponding two-photon state can be derived by first-order perturbation theory and, under the assumption of a quasi-monochromatic pump field, is described by

$$|\psi\rangle = \int_{-\infty}^{\infty} d\omega \Lambda(\omega) \hat{a}_i^\dagger(\omega) \hat{a}_s^\dagger(-\omega) |0\rangle_i |0\rangle_s, \quad (7)$$

where we omit the leading order vacuum state. Signal and idler photons are created with corresponding relative frequency ω by acting with the operators $\hat{a}_{i,s}^\dagger(\omega)$ on the composite vacuum state $|0\rangle_i |0\rangle_s$. The joint spectral amplitude reads

$$\Lambda(\omega) \propto \text{sinc} \left[\frac{\left(\Delta k_{DC}(\omega) + \frac{2\pi}{G_{DC}} \right) L_{DC}}{2} \right], \quad (8)$$

where the phase mismatch $\Delta k_{DC}(\omega)$ is responsible for the efficiency of the SPDC process and includes the dispersion properties of the down-conversion crystal through its corresponding Sellmeier equations.

To manipulate their spectrum, the entangled photons are imaged from the SPDC crystal through a four-prism compressor (P1-P4) to the plane Σ_2 . The prism compressor consists of four equilateral N-SF 11 prisms arranged in minimum deviation geometry. The lens L1 images the plane Σ_0 to Σ_1 such that the spectral components are spatially dispersed in order to form a quasi-Fourier plane. Placing a spatial light modulator (SLM, Jenoptik SLM-S640d) at Σ_1 then allows to individually manipulate the spectral amplitude and phase of the entangled photons similar to pulse shaping techniques applied to classical femtosecond laser pulses [31]. The effect of the SLM on each photon is described by a complex transfer function $M^{i,s}(\omega)$ which transforms the joint spectral amplitude of Eq. (8) according to

$$\tilde{\Lambda}(\omega) = M(\omega) \Lambda(\omega) \quad (9)$$

with

$$M(\omega) = M^i(\omega) M^s(-\omega). \quad (10)$$

Instead of using two spatially separated single-photon detectors, coincidences of the entangled photon pairs are measured by SFG in a second PPKTP crystal with length $L_{SFG} = 11.5$ mm and poling period $G_{SFG} = 9$ μm . This ensures an ultrafast coincidence window with femtosecond temporal resolution needed to observe a coherent superposition of entangled photons with different energies. To take account of the detection crystals acceptance bandwidth, we define the modified joint spectral amplitude

$$\Gamma(\omega) \propto \Lambda(\omega) \Phi(\omega) \quad (11)$$

with

$$\Phi(\omega) = \text{sinc} \left[\frac{\left(\Delta k_{SFG}(\omega) - \frac{2\pi}{G_{SFG}} \right) L_{SFG}}{2} \right] \quad (12)$$

and $\Delta k_{SFG}(\omega)$ now being the phase mismatch responsible for the efficiency of the SFG process. The recombined 532 nm photons are then imaged onto the photosensitive area of a SPCM (IDQ id100-50). In order to exclude the detection of residual infrared photons we mounted a bandpass filter in front of lens L4. The SFG signal S is in general proportional to

$$S \propto \left| \int_{-\infty}^{\infty} d\omega M(\omega) \Gamma(\omega) \right|^2. \quad (13)$$

However, diffraction effects due to the finite aperture of the lenses and prisms lead to a point-to-spot image from Σ_0 to Σ_1 . Therefore, a given frequency component is blurred over several pixels of the SLM. This effect is taken into account by a convolution of $\Gamma(\omega)$ with a Gaussian-shaped point spread function $PSF(\omega)$, i.e.,

$$\Gamma(\omega) \rightarrow \Gamma_{PSF}(\omega) \propto (\Gamma \otimes PSF)(\omega). \quad (14)$$

We encode qudits in the frequency domain by projecting the continuous state $|\psi\rangle$ of Eq. (7) into a discrete d^2 -dimensional subspace spanned by frequency-bin states $|j\rangle_i |k\rangle_s$ with $|j\rangle_{i,s} \equiv \int_{-\infty}^{\infty} d\omega f_j^{i,s}(\omega) \hat{a}_{i,s}^\dagger(\omega) |0\rangle_{i,s}$ and $j = 0, \dots, d-1$. The frequency bins itself are defined according to

$$f_j^{i,s}(\omega) = \begin{cases} 1/\sqrt{\Delta\omega_j} & \text{for } |\omega - \omega_j| < \Delta\omega_j/2, \\ 0 & \text{otherwise,} \end{cases} \quad (15)$$

and are represented in Figure 2 together with a measured SPDC spectrum. Furthermore, imposing of the constraint $|\omega_j - \omega_k| > (\Delta\omega_j + \Delta\omega_k)/2$ for all j, k ensures

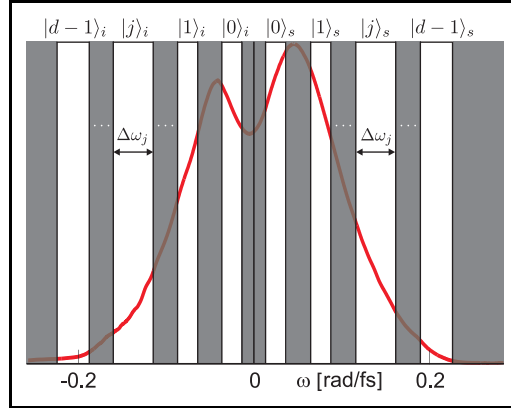


Figure 2. Measured SPDC spectrum overlaid with a schematic frequency-bin pattern. The transmitted amplitude $|u_j^{i,s}|$ (white bars) of each bin can be adjusted through amplitude modulation by means of the SLM.

that adjacent bins do not overlap. Under the restriction of a monochromatic pump

field, the projected state is expressed as

$$|\psi\rangle^{(d)} = \sum_{j=0}^{d-1} c_j |j\rangle_i |j\rangle_s \quad (16)$$

with amplitudes $c_j = \int_{-\infty}^{\infty} d\omega f_j^i(\omega) f_j^s(-\omega) \Gamma(\omega)$. The frequency-bin structure of Eq. (15) is applied on the SLM by the transfer function

$$M^{i,s}(\omega) = \sum_{j=0}^{d-1} u_j^{i,s} f_j^{i,s}(\omega) = \sum_{j=0}^{d-1} |u_j^{i,s}| e^{i\phi_j^{i,s}} f_j^{i,s}(\omega), \quad (17)$$

where the amplitude $|u_j^{i,s}|$ and phase $\phi_j^{i,s}$ of bin j is controlled independently. Since in our experiment there is no spatial separation between idler and signal modes, we address each photon individually by assigning $M^i(\omega)$ to the lower-frequency part and $M^s(\omega)$ to the higher-frequency part of the spectrum. In fact, due to the PSF, we do have a small overlap between the spectral components of the idler and the signal domain such that the two spaces cannot be considered completely independent of one another. The measured signal of Eq. (13) is equivalent to the projection

$$S = \left| \langle \chi | \psi \rangle^{(d)} \right|^2 = \left| \sum_{j=0}^{d-1} u_j^i u_j^s c_j \right|^2 \quad (18)$$

for a direct product state

$$|\chi\rangle = \left(\sum_{j=0}^{d-1} u_j^{i*} |j\rangle_i \right) \left(\sum_{j'=0}^{d-1} u_{j'}^{s*} |j'\rangle_s \right) \quad (19)$$

and a decomposition of the transfer function according to Eq. (17). The combination of the SLM together with an SFG coincidence detection therefore realizes a projective measurement. Different quantum-information protocols can thus be implemented through a judicious choice of $|\chi\rangle$ together with Eq. (17). The state of Eq. (19) can, for instance, be chosen in the form of a tomographically complete set to perform quantum state reconstruction of maximally entangled qudits up to $d = 4$ as demonstrated in [7]. Here, Eq.(19) serves to perform Bell measurements for maximally and non-maximally entangled qutrits. If we identify $i \leftrightarrow A$ and $s \leftrightarrow B$, the Bell parameter of Eq. (6) is described by a combination of projective measurements onto the state of Eq. (19) expressed as $|\chi_{a,b}\rangle = |a\rangle_A^x |b\rangle_B^y$, and defined by

$$|a\rangle_A^x = \frac{1}{\sqrt{3}} \sum_{j=0}^2 \exp\left(i\frac{2\pi}{3}j(a + \alpha_x)\right) |j\rangle_A, \quad (20)$$

$$|b\rangle_B^y = \frac{1}{\sqrt{3}} \sum_{j=0}^2 \exp\left(i\frac{2\pi}{3}j(-b + \beta_y)\right) |j\rangle_B, \quad (21)$$

with $a, b = 0, 1, 2$ for a specific choice of detection settings $\alpha_1 = 0, \alpha_2 = 1/2, \beta_1 = 1/4$, and $\beta_2 = -1/4$ according to [13]. Note, that these settings are only optimal in the

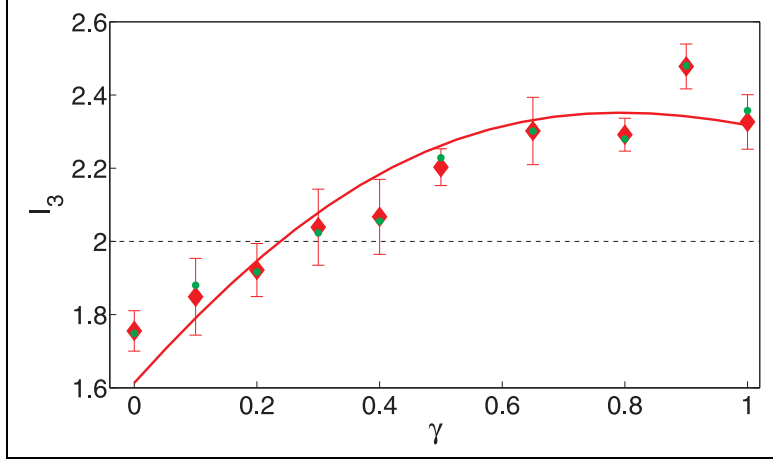


Figure 3. Bell parameter $I_3(\gamma)$. The experimental Bell parameter $I_3^{\text{expt.}}$ is depicted with red diamonds. The 2σ uncertainties are calculated assuming Poisson statistics on background-subtracted coincidence counts. The theoretically predicted Bell parameter $I_3(\gamma)$ (solid red line) is scaled with its corresponding mixing parameter. The (horizontal) dashed black line indicates the local variable realistic. We experimentally determine the mixing parameter to be $\lambda_3^{\text{expt.}} = 0.807 \pm 0.008$ with 2σ uncertainties. The green dots represent $I_3^{\text{expt.}}$ with signaling revised experimental data (discussion Section 4.2).

case of $\gamma = 1$ and $\gamma = \gamma_{\max}$ [1]. Allowing for the state of Eq. (4), the individual joint probabilities become a function of γ . In accordance with Eq. (18), a measured coincidence signal is then given by

$$P_\gamma(A_x = a, B_y = b) \propto \left| \langle \chi_{a,b} | \psi(\gamma) \rangle^{(3)} \right|^2 \quad (22)$$

with the projection states of Eq. (20) and (21). Starting from a maximally entangled state through Procrustean filtering [6], the reduced entanglement, i.e., $\gamma < 1$, is obtained by decreasing the transmission amplitudes $|u_1^i|$ and $|u_1^s|$ of the bins associated with $|1\rangle_A |1\rangle_B$ using the SLM. The experimental data $I_3^{\text{expt.}}(\gamma)$ (red diamonds) are depicted in Figure 3 together with the theoretical result for $I_3(\gamma)$ (solid red line). The latter is scaled to the measured data using a symmetric noise model $\hat{\rho}^{(d)} = \lambda_d |\psi\rangle^{(d)} \langle \psi| + (1 - \lambda_d) \mathbb{1}_{d^2}/d^2$, where the mixing parameter λ_d quantifies the deviations from a pure state and $\mathbb{1}_{d^2}$ denotes a d^2 -dimensional identity operator. Under the given measurement settings together with white noise and possible misalignments in the experimental setup Figure 3 demonstrates a violation of Eq. (5) for $\gamma \geq 0.5$.

3. Measures of Non-Locality

3.1. Systems and correlations

The goal of the experiment discussed in this article is to understand and quantify *correlations* that occur when two parts of a physical system in a common state are measured. More precisely, this type of correlation displays itself in the behavior of a *system*, i.e., a joint input-output behavior.

Definition 1 A two-party *input-output behavior* or *system* is a conditional probability distribution $P(ab|xy)$, where x and y are the respective inputs of the two parties and a and b are their outputs.

A *two-partite quantum state* is a natural way to obtain a system: Given a set of possible alternative measurements (x and y) to be carried out by the two parties, their outcomes (a and b) correspond to the outputs of the system. We establish a general framework for studying such systems, and for quantifying their non-locality, independently of whether they come from a quantum state or not.

Classically speaking, the two players not allowed to communicate can, for obtaining a given joint behavior, apply *local strategies*. Generally, such a strategy can employ local randomness and even shared (classical) information.

Definition 2 Two players' *local strategies* are ways of determining their respective outputs as a function of their inputs. A *local strategy (for the first player)* is of the form $a = f(x, L, R)$, where f is a function, L is a classical random variable and R is a shared (i.e., also known to the other player) random variable. As a special case, a strategy is *local deterministic* if it is of the form $a = f(x)$ for some fixed function f .

A system that cannot be simulated by any pair of local strategies is called non-local. Such systems are, in classical terms, only explainable by *communication*. It is important to note, however, that this does not mean that any non-local system *allows* for such communication. Actually, our focus is precisely on the systems which are non-local yet non-signaling at the same time.

Definition 3 A two-partite system is *local* if it can be simulated by two players using a pair of local strategies. It is *non-signaling* if the output of a party, given its input, is independent of the input of the other party: We have $P(a|xy) = P(a|x)$, and *vice versa*.

It is the goal of the rest of this section to identify criteria for testing whether a (non-signaling) system is local or not and, if not, to give a measure for the strength or amount of non-locality it displays. Whereas the violation of a fixed Bell inequality is a sufficient criterion for non-locality, it is *not necessary*. In the same sense, the extent by which a given inequality is violated does not directly measure non-locality. We describe two criteria and measures: The first corresponds, in a sense, to taking *all* Bell inequalities into account, whereas the second is of different nature and based on the price, measured in terms of classical communication, one has to pay for establishing a correlation.

3.2. Distance to the polytope of local correlations

Within the space of non-signaling two-party systems, the *local* systems form a subset or, more precisely, a *convex polytope*, somewhat abusively called the *local polytope*. Whereas Bell inequalities characterize this polytope in terms of its *facets*, we can also do the same through its extremal points, which correspond to the *local deterministic strategies*; every local strategy is a convex combination of local deterministic strategies. We use this description as a locality test as well as a quantification of the non-local content of a given, e.g., experimentally observed, system.

For a system $P(ab|xy)$, we denote by $|a|$, $|b|$, $|x|$, and $|y|$ the sizes of the ranges of the corresponding random variables. A pair of strategies can be represented in the $(|a||x||b||y|)$ -dimensional real space. The number of pairs of local deterministic

strategies is $|a|^{|x|}|b|^{|y|}$. Now, any local (probabilistic) strategy is a (non-trivial) convex combination of local deterministic strategies. We check whether an observed behavior lies inside this polytope, and if not, we calculate the distance to this polytope in the L^1 norm, using *linear programming* [15, 17], by minimizing the difference between the given behavior and a local approximation of it. The larger this distance, the stronger a behavior can be considered non-local. More specifically, the fact that a behavior has non-zero distance to the polytope can indicate that it violates a Bell inequality *or* that it is signaling (or both).

3.3. The amount of communication required for establishing correlations

A non-locality measure alternative to Bell-inequality or polytope-distance based measures uses the fact that the local correlations are exactly the ones that can, classically speaking, be explained by shared information and require *no* communication. Hence, a non-locality measure is given by the *minimal amount* of classical communication required to simulate the correlations. In [23], this measure has been called *non-local capacity*. There, it was proven that the non-local capacity is the minimum of a convex functional over a suitable space of probability distributions, so that its computation is a convex-optimization problem. We review that method, which we apply for calculating the non-local capacity from the experimental data.

3.3.1. Communication cost and non-local capacity. A general classical simulation of correlations $P(ab|xy)$ employing a one-way communication between the two parties is as follows. A party, say Alice, chooses the input x corresponding to the measurement she wants to simulate. She generates a variable k and the measurement outcome a according to a conditional probability distribution $P(ak|xr)$ depending on the input x and a random variable R shared with the other party, say Bob, and generated with probability distribution $\rho(R)$. Then, she sends k to Bob. Finally, Bob chooses the measurement he wants to simulate, labelled by the index y , and generates an outcome B according to a conditional probability distribution $\rho(b|ykr)$. The protocol exactly simulates the correlations $P(ab|xy)$ if

$$\sum_k \int dr P(b|ykr) P(ak|xr) \rho(r) = P(ab|xy) . \quad (23)$$

There are different definitions of communication cost of a simulation. We could define the communication cost as the number of required bits in the worst case, or as the average number of bits. As done in [23], we employ the entropic definition and we define the communication cost, say \mathcal{C} , as the maximum, over the space of distributions $P(a)$, of the conditional Shannon entropy $H(K|Y) \equiv - \int dr \rho(r) \sum_k P(k|r) \log_2 P(k|r)$. That is,

$$\mathcal{C} \equiv \max_{P(x)} H(K|R) . \quad (24)$$

We define the *non-local capacity*, denoted by \mathcal{C}_{nl} , of the correlations $P(ab|xy)$ as the minimal amount of communication \mathcal{C} required for an exact simulation of them. More generally, we can perform a parallel simulation of N distinct pairs of entangled systems. We define the *asymptotic communication cost*, denoted by \mathcal{C}^{asym} , as the communication cost of the simulation divided by N , in the limit $N \rightarrow \infty$ (see [23] for a more detailed definition). The asymptotic non-local capacity, denoted by \mathcal{C}_{nl}^{asym} , is defined as the minimum of \mathcal{C}^{asym} over the class of parallel simulations.

3.3.2. A convex-optimization problem. In the following, we assume that Bob can choose a measurement among a finite set of possibilities. The index y can take values from 1 to M . In [23], it was shown that the asymptotic non-local capacity is the minimum of a convex functional over a suitable space of probability distributions \mathcal{V} .

Definition 4 Given a non-signaling system $P(ab|xy)$, the set \mathcal{V} contains any conditional probability $\rho(a\mathbf{b}|x)$ over a and the sequence $\mathbf{b} = (b_1, \dots, b_M)$ whose marginal distribution of a and the m -th variable is the distribution $P(ab|x, y = m)$.

In other words, \mathcal{V} contains any $\rho(a\mathbf{b}|x)$ satisfying the constraints

$$\sum_{\mathbf{b}, b_m=b} \rho(x\mathbf{b}|x) = P(ab|x, y = m) , \quad (25)$$

where

$$\sum_{\mathbf{b}, b_m=b} \rightarrow \sum_{b_1, \dots, b_m=b, \dots, b_M} \quad (26)$$

is the summation over every index in \mathbf{b} but the m -th one, which is set equal to b .

We proved that

$$\mathcal{C}_{nl}^{asym} = \min_{\rho(a\mathbf{b}|x) \in \mathcal{V}} \mathcal{C}(x \rightarrow \mathbf{b}) , \quad (27)$$

where

$$\mathcal{C}(a \rightarrow \mathbf{b}) \equiv \max_{\rho(x)} I(\mathbf{b}; x) \quad (28)$$

is the capacity of the channel $\rho(\mathbf{b}|x)$. Let us recall that the capacity of a channel $a \rightarrow \mathbf{b}$ is the maximum of the mutual information $I(\mathbf{b}; x)$ between the input and the output over the space of input probability distributions $\rho(x)$ [14]. As the mutual information is convex and the maximum over a set of convex functions is still convex [8], the asymptotic communication complexity is the minimum of a convex function over the space \mathcal{V} . Furthermore, the equality constraints defining the set \mathcal{V} are linear. This implies that the minimization problem is convex and can be numerically solved with standard methods [8].

4. Analysis of Experimental Data

4.1. The raw data display signaling

We analyze the experimentally obtained two-partite system according to Eq. (22). A first remarkable result of our analysis of this system is that it happens to be, actually, not only non-local but even *signaling*. From the point of view of how the qutrits were experimentally realized (not spatially separated), this is not overly surprising and, in particular, not in violation of relativity. In order to be able to apply the non-locality quantification, designed for non-signaling systems, to the data, we free them of their signaling part, replacing them by the closest respective non-signaling systems. Figure 4 demonstrates that for $\gamma < 0.2$, the resulting non-signaling systems end up being local, whereas for $\gamma \geq 0.5$, there is no significant difference between the raw and the corrected data.

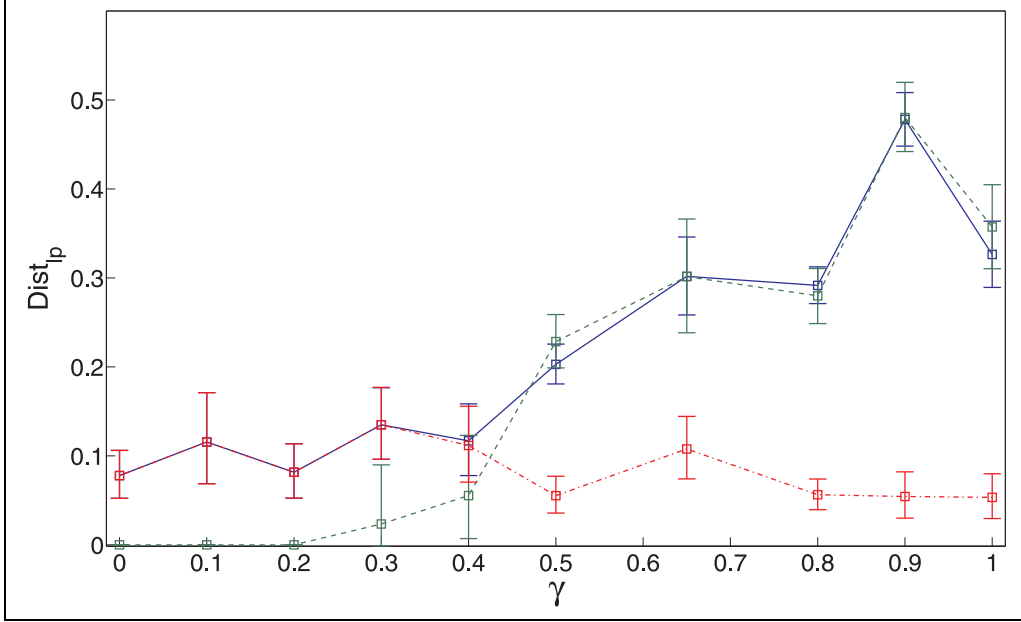


Figure 4. The distance to the local polytope ($Dist_{lp}$) before (blue squares) and after (green squares) removing the signaling part, and the distance to the non-signaling polytope (red squares). The corresponding lines (solid blue, dashed green, dot-dashed red) are guides to the eyes.

4.2. Removal of the signaling part

Removing the signaling part in the described way can be seen as some kind of error correction; after all, we know that quantum theory is, despite the phenomena of entanglement and non-locality, non-signaling. The computation of the non-signaling part is performed similarly to the computation of the distance to the polytope, where in this case, the *non-signaling polytope* instead of the local polytope is used. Our method of getting rid of experimental errors is similar to a procedure discussed in the literature [11] that proposes a maximum-likelihood estimation from the set of all quantum states. We adapt the method for non-signaling systems instead of physical states. Note that while the removal of the signaling part can greatly influence the measures for non-locality used here, it has almost no influence on Bell-inequality violations (Figure 3).

4.3. Comparison between the two methods

First, we observe that the two non-locality measures behave very similarly for the investigated measurement data (Figure 5). Second, we can conclude from our analysis that the *non-monotonicity* of the measured non-locality as compared to the *entanglement* — a phenomenon already reported previously in the context of non-maximally entangled qubit pairs [10] — is not merely an effect that is respective to a single (strange) Bell inequality, but that persists also with respect to the non-locality measures.

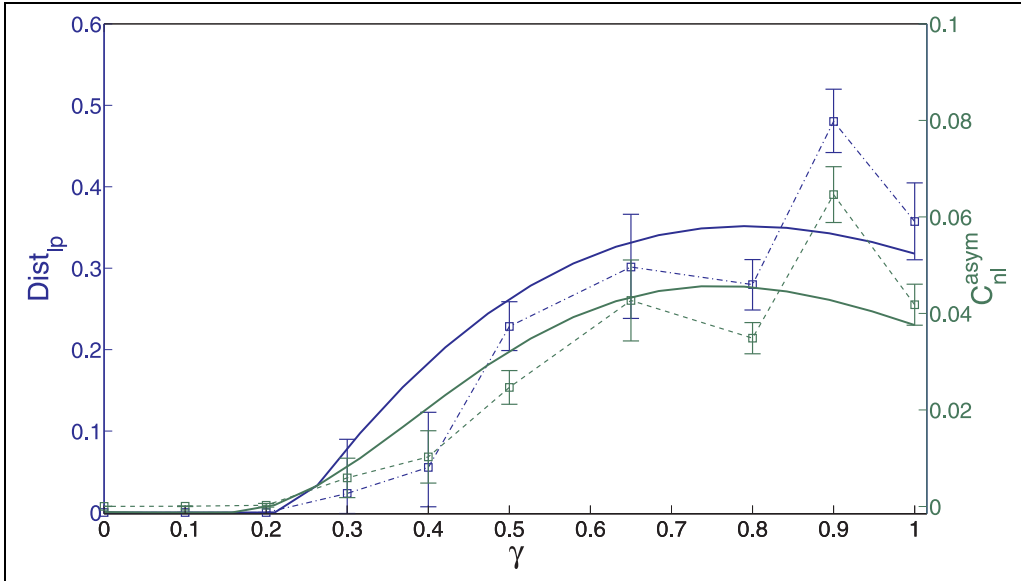


Figure 5. Two alternative methods for quantifying non-locality are compared to each other. The blue squares with the blue scale on the left show the distance to the local polytope ($Dist_{lp}$), whereas the green squares with the green scale on the right show the asymptotic non-local capacity (C_{nl}^{asym}). The corresponding lines (dot-dashed blue, dashed green) are guides to the eyes. Theoretical values for $Dist_{lp}$ and C_{nl}^{asym} are indicated with solid lines (upper blue, lower green).

5. Concluding Remarks

In this article, dedicated to the celebration of the 50th anniversary of John Stewart Bell’s famous and seminal theorem, we have described an experiment for measuring the non-locality of entangled qutrit pairs. We have analyzed the resulting experimental data, and in particular the strength of their non-locality, with two non-standard methods, namely the distance to the local polytope (in the space of non-signaling behaviors) as well as the communication cost for classically simulating the correlations.

In the results presented here, there is no difference between the non-local content as measured by the Bell parameter compared to the alternative methods, i.e., the distance to the local polytope and the non-local capacity. This is because the measurement settings are chosen in order to strongly violate a specific Bell inequality. However, for an arbitrary state for which the optimal Bell inequality is not known, the alternative methods offer a more effective way of testing non-locality, by performing less measurements.

The phenomenon of non-locality, John Bell’s profound discovery, continues to put into question the way we traditionally view space and time. When one tries to understand — just as Bell himself did in a number of articles [5] — non-locality in the context of different interpretations of quantum theory, the conclusion is always the same: It does not fit. In collapse theories, how can spontaneously generated information be identical in different spatial positions? In modern deterministic theories such as the “church of the larger Hilbert space,” parallel universes or “parallel lives” [9], no mechanism that could *explain* the correlations has been described. It appears that

the interpretation which passes the “Bell test” and is suitable for embedding, in a non-artificial way, non-local correlations is yet to be found. It may have the property that space and time, in particular spatial distance and spacelike separation, do not exist prior to, but only emerge *together* with the (correlated) classical information.

Acknowledgements. This research was supported by the Swiss National Science Foundation (SNF), the NCCR *QSIT*, the NCCR *MUST*, the SNF Grant No. PP00P2_133596, the COST action on “Fundamental Problems in Quantum Physics,” and the CHIST-ERA *DIQIP*.

- [1] Antonio Acín, Thomas Durt, Nicolas Gisin, and José I Latorre. Quantum nonlocality in two three-level systems. *Physical Review A*, 65:052325, 2002.
- [2] Alain Aspect, Jean Dalibard, and Gérard Roger. Experimental test of Bell’s inequalities using time-varying analyzers. *Physical Review Letters*, 49(25):1804–1807, 1982.
- [3] Tomer J Barnea, Jean-Daniel Bancal, Yeong-Cherng Liang, and Nicolas Gisin. A tripartite quantum state violating the hidden influence constraints. *Physical Review A*, 88:022123, 2013.
- [4] John S Bell. On the Einstein-Podolsky-Rosen paradox. *Physics*, 1:195–200, 1964.
- [5] John S Bell. *Speakable and Unspeakable in Quantum Mechanics: Collected Papers on Quantum Philosophy*. Cambridge University Press, 2004.
- [6] Charles H Bennett, Herbert J Bernstein, Sandu Popescu, and Benjamin Schumacher. Concentrating partial entanglement by local operations. *Physical Review A*, 53(4):2046, 1996.
- [7] Christof Bernhard, Bänz Bessire, Thomas Feurer, and André Stefanov. Shaping frequency-entangled qudits. *Physical Review A*, 88:032322, 2013.
- [8] Stephen Boyd and Lieven Vandenberghe. *Convex Optimization*. Cambridge University Press, 2004.
- [9] Gilles Brassard and Paul Raymond-Robichaud. Can free will emerge from determinism in quantum theory? In *Is Science Compatible with Free Will?*, pages 41–61. Springer, 2013.
- [10] Nicolas Brunner, Nicolas Gisin, and Valerio Scarani. Entanglement and non-locality are different resources. *New Journal of Physics*, 7(1):88, 2005.
- [11] Matthias Christandl and Renato Renner. Reliable quantum state tomography. *Physical Review Letters*, 109(12):120403, 2012.
- [12] John F Clauser, Michael A Horne, Abner Shimony, and Richard A Holt. Proposed experiment to test local hidden-variable theories. *Physical Review Letters*, 23(15):880–884, 1969.
- [13] Daniel Collins, Nicolas Gisin, Noah Linden, Serge Massar, and Sandu Popescu. Bell inequalities for arbitrarily high dimensional systems. *Physical Review Letters*, 88(4):040404, 2002.
- [14] Thomas M Cover and Joy A Thomas. *Elements of Information Theory (Wiley Series in Telecommunications and Signal Processing)*. Wiley-Interscience, 2006.
- [15] George B Dantzig. *Linear programming and extensions*. Princeton university press, 1965.
- [16] Barak Dayan, Avi Peer, Asher A Friesem, and Yaron Silberberg. Nonlinear interactions with an ultrahigh flux of broadband entangled photons. *Physical Review Letters*, 94(4):043602, 2005.
- [17] Matthew B Elliott. A linear program for testing local realism. *arXiv preprint arXiv:0905.2950*, 2009.
- [18] Stuart J Freedman and John F Clauser. Experimental test of local hidden-variable theories. *Physical Review Letters*, 28(14):938–941, 1972.
- [19] Marissa Giustina et al. Bell violation using entangled photons without the fair-sampling assumption. *Nature*, 497(7448):227–230, 2013.
- [20] Julian Hofmann, Michael Krug, Norbert Ortegel, Lea Gérard, Markus Weber, Wenjamin Rosenfeld, and Harald Weinfurter. Heralded entanglement between widely separated atoms. *Science*, 337(6090):72–75, 2012.
- [21] Ryszard Horodecki, Paweł Horodecki, and Michał Horodecki. Violating Bell inequality by mixed spin- $\frac{1}{2}$ states: Necessary and sufficient condition. *Physics Letters A*, 200(5):340–344, 1995.
- [22] Simon Kochen and Ernst Specker. The problem of hidden variables in quantum mechanics. In *The Logico-Algebraic Approach to Quantum Mechanics*, pages 293–328. Springer, 1975.
- [23] Alberto Montina and Stefan Wolf. Information-based measure of nonlocality. *arXiv preprint arXiv:1312.6290*, 2013.
- [24] Renato Renner and Stefan Wolf. Quantum pseudo-telepathy and the Kochen-Specker theorem. In *IEEE International Symposium on Information Theory*, pages 322–322, 2004.

- [25] Mary A Rowe, David Kielpinski, V Meyer, Charles A Sackett, Wayne M Itano, Christopher Monroe, and David J Wineland. Experimental violation of a Bell's inequality with efficient detection. *Nature*, 409(6822):791–794, 2001.
- [26] Daniel Salart, Augustin Baas, Cyril Branciard, Nicolas Gisin, and Hugo Zbinden. Testing the speed of spooky action at a distance. *Nature*, 454(7206):861–864, 2008.
- [27] André Stefanov, Hugo Zbinden, Nicolas Gisin, and Antoine Suarez. Quantum correlations with spacelike separated beam splitters in motion: Experimental test of multisimultaneity. *Physical Review Letters*, 88(12):120404, 2002.
- [28] Wolfgang Tittel, Juergen Brendel, Hugo Zbinden, and Nicolas Gisin. Violation of Bell inequalities by photons more than 10 km apart. *Physical Review Letters*, 81(17):3563, 1998.
- [29] Rupert Ursin et al. Entanglement-based quantum communication over 144 km. *Nature Physics*, 3(7):481–486, 2007.
- [30] Gregor Weihs, Thomas Jennewein, Christoph Simon, Harald Weinfurter, and Anton Zeilinger. Violation of Bell's inequality under strict Einstein locality conditions. *Physical Review Letters*, 81(23):5039, 1998.
- [31] Andrew M Weiner. Femtosecond pulse shaping using spatial light modulators. *Review of Scientific Instruments*, 71(5):1929–1960, 2000.
- [32] Thomas P Wihler, Bänz Bessire, and André Stefanov. Computing the entropy of a large matrix. *arXiv preprint arXiv:1209.2575*, 2012.
- [33] Stefan Zohren and Richard D Gill. Maximal violation of the Collins-Gisin-Linden-Massar-Popescu inequality for infinite dimensional states. *Physical Review Letters*, 100(12):120406, 2008.